

Heavy element nucleosynthesis: the r process

Gabriel Martínez Pinedo



TECHNISCHE
UNIVERSITÄT
DARMSTADT

55th Karpacz Winter School of Theoretical Physics
ChETEC COST Action CA16117 training school
Artus Hotel, Karpacz, February 24 - March 2, 2019

HELMHOLTZ
RESEARCH FOR GRAND CHALLENGES



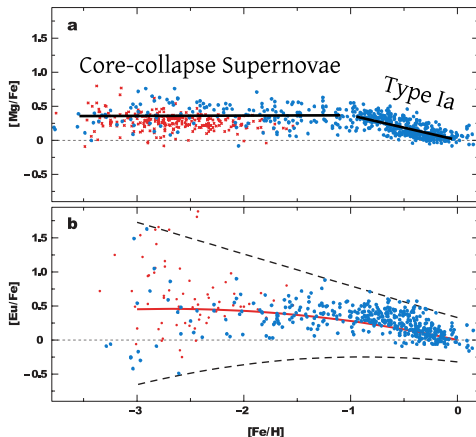
DFG

Outline

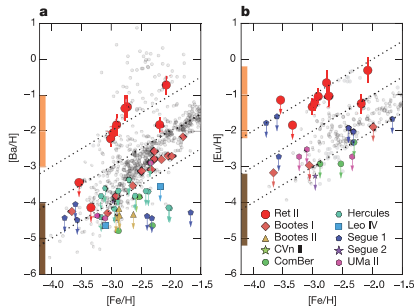
- 1 Signatures of heavy element nucleosynthesis
- 2 Basic concepts Astrophysical reaction rates
- 3 General working of the r process
- 4 r process in mergers
- 5 Summary

Implications from observations

Individual stars, Milky Way Halo
Snedden, Cowan & Gallino, 2008



Ji et al 2016 found that only 1 of 10 ultrafaint dwarf galaxies is enriched in r-process elements

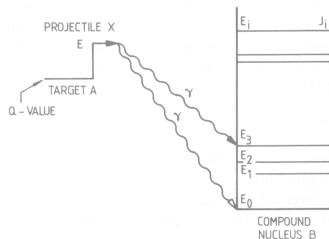
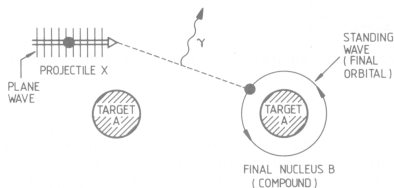


R process related to rare high yield events not correlated with Iron enrichment

Similar results obtained by ^{60}Fe and ^{244}Pu observations in deep sea sediments (Wallner et al, 2015; Hotokezaka et al, 2015)

Direct reactions

So far we have discussed the so-called “direct reactions” in which the reaction proceeds directly to a bound nuclear state:



Resonance cross section

The cross section for capture through an isolated resonance is given by the Breit-Wigner formula:



$$\sigma(E) = \pi \lambda^2 \frac{(2J_C + 1)(1 + \delta_{aA})}{(2J_a + 1)(2J_A + 1)} \frac{\Gamma_{aA} \Gamma_{bB}}{(E - E_r)^2 + (\Gamma/2)^2}, \quad \lambda = \frac{1}{k} = \frac{\hbar}{p}$$

with $\Gamma = \Gamma_{aA} + \Gamma_{bB} + \dots$ (sum over all partial widths for all possible decay channels). They depend on energy.

Particle width For charged particles is strongly dependent on energy due to tunneling through coulomb barrier.

Photon width Depends on the so called gamma strength function (will be discussed later)

Hauser-Feshbach cross section and reaction rate

Christian Iliadis, *Nuclear Physics of Stars*

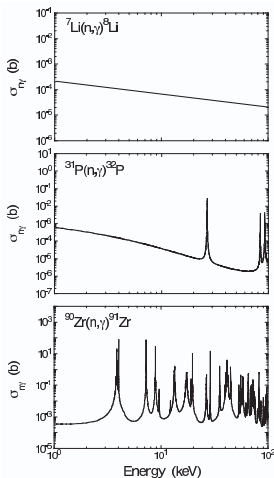


Fig. 3.30 Cross sections for neutron capture on ${}^7\text{Li}$, ${}^{31}\text{P}$, and ${}^{90}\text{Zr}$ versus energy. The curve in the upper panel shows a $1/v$ behavior, while resonances are visible in the middle and lower panels.

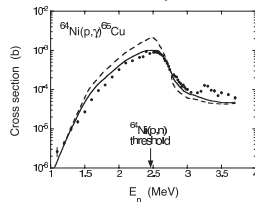


Fig. 2.29 Cross section versus bombarding energy for the ${}^{64}\text{Ni}(p,\gamma){}^{65}\text{Cu}$ reaction. Beyond an energy of ≈ 2.5 MeV the endothermic ${}^{64}\text{Ni}(p,n){}^{65}\text{Cu}$ reaction is energetically allowed. The sharp drop in the cross section at the neutron threshold reflects the decrease of the flux in all other decay channels of the compound nucleus ${}^{65}\text{Cu}$.

The curves show the results of Hauser-Feshbach statistical model calculations with (solid line) and without (dashed line) width fluctuation corrections. Reprinted from F. M. Mann et al., *Phys. Lett. B*, Vol. 58, p. 420 (1975). Copyright (1975), with permission from Elsevier.

- With increasing mass number reactions are determined by a larger number of resonances
- Often it is not possible to experimentally resolve resonances. Astrophysical reaction rate is an energy average over many resonances.
- Hauser-Feshbach provides and statistically averaged cross section from the contribution of many resonances in an energy interval.

Hauser-Feshbach cross section

The Hauser-Feshbach expression for the cross section of an (n, γ) reaction proceeding from the target nucleus i in the state μ with spin J_i^μ and parity π_i^μ to a final state ν with spin J_m^ν and parity π_m^ν in the residual nucleus m via a compound state with excitation energy E , spin J , and parity π is given by

$$\sigma_{(n,\gamma)}^{\mu\nu}(E_{i,n}) = \frac{\pi \hbar^2}{2M_{i,n} E_{i,n}} \frac{1}{(2J_i^\mu + 1)(2J_n + 1)} \sum_{J,\pi} (2J + 1) \frac{T_n^\mu T_\gamma^\nu}{T_n^\mu + T_\gamma^\nu}$$

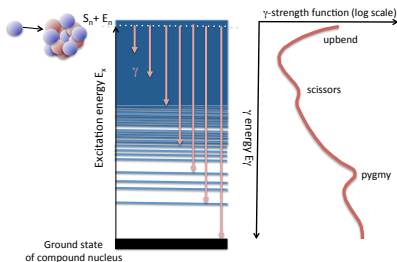
where $E_{i,n}$ and $M_{i,n}$ are the center-of-mass energy and the reduced mass for the initial system. $J_n = 1/2$ is the neutron spin. Normally we have situations in which $T_n \gg T_\gamma$. The transmission coefficients, multipolarity XL , are related to the average decay width and level density (ρ) or the gamma strength function, f_{XL} :

$$T_{XL} = 2\pi\rho \langle \Gamma_{XL} \rangle = 2\pi E_\gamma^{2L+1} f_{XL}$$

Structure dipole gamma-strength function

The gamma-decay is dominated by dipole transitions. Total transmission coefficient (sum final bound states)

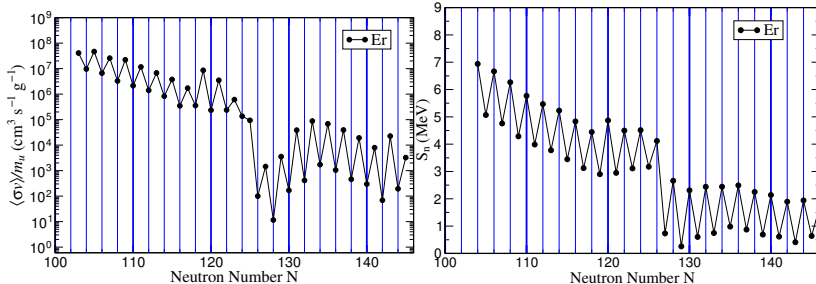
$$T_1 = \sum_{\nu} 2\pi E_{\gamma}^3 f_{1,\nu} = 2\pi \int E_{\gamma}^3 f_1(E_{\gamma}) \rho(E_{\gamma}) dE_{\gamma}$$



Favored decay energy determined by a competition between level density, ρ , and gamma-strength function.

Systematics $\langle\sigma v\rangle$ and neutron separation energies

Neutron capture rates reflect the behavior of neutron separation energies



Inverse reactions

Let's have the reaction



We are interested in the inverse reaction. One can use detailed-balance to determine the inverse rate. Simpler using the concept of chemical equilibrium.

$$\frac{dn_a}{dt} = -n_a n_A \langle \sigma v \rangle_{aA} + (1 + \delta_{aA}) n_B \lambda_\gamma = 0$$

$$\left(\frac{n_a n_A}{n_B} \right)_{\text{eq}} = (1 + \delta_{aA}) \frac{\lambda_\gamma}{\langle \sigma v \rangle_{aA}}$$

Using equilibrium condition for chemical potentials: $\mu_a + \mu_A = \mu_B$

$$\mu(Z, A) = m(Z, A)c^2 + kT \ln \left[\frac{n(Z, A)}{G_{(Z,A)}(T)} \left(\frac{2\pi\hbar^2}{m(Z, A)k_B T} \right)^{3/2} \right], \quad G_{(Z,A)}(T) = \sum_i (2J_i + 1) e^{-E_i/(kT)}$$

Inverse reactions

One obtains:

$$\left(\frac{n_a n_A}{n_B}\right)_{\text{eq}} = \frac{G_a G_A}{G_B} \left(\frac{m_a m_A}{m_B}\right)^{3/2} \left(\frac{k_B T}{2\pi\hbar^2}\right)^{3/2} e^{-Q/k_B T}$$

Finally, we obtain:

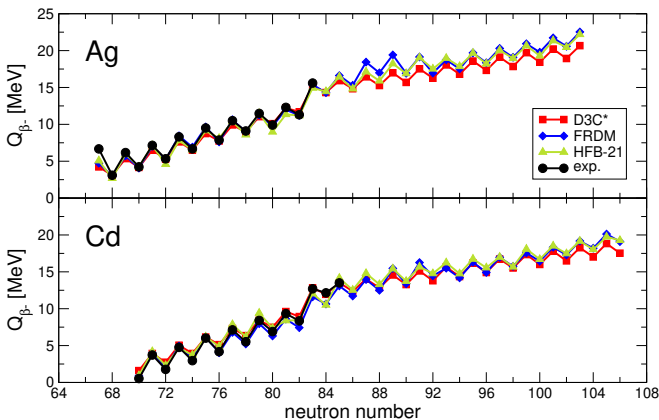
$$\lambda_\gamma = \frac{G_a G_A}{(1 + \delta_{aA}) G_B} \left(\frac{m_a m_A}{m_B}\right)^{3/2} \left(\frac{k_B T}{2\pi\hbar^2}\right)^{3/2} e^{-Q/k_B T} \langle\sigma v\rangle$$

For a reaction $a + A \rightarrow B + b$ ($Q = m_a + m_A - m_B - m_b$):

$$\langle\sigma v\rangle_{bB} = \frac{(1 + \delta_{bB}) G_a G_A}{(1 + \delta_{aA}) G_b G_B} \left(\frac{m_a m_A}{m_b m_B}\right)^{3/2} e^{-Q/k_B T} \langle\sigma v\rangle_{aA}$$

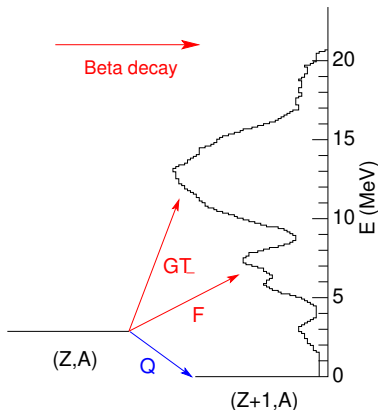
Systematics beta-decay Q -values

The decay Q -value increases with neutron excess.



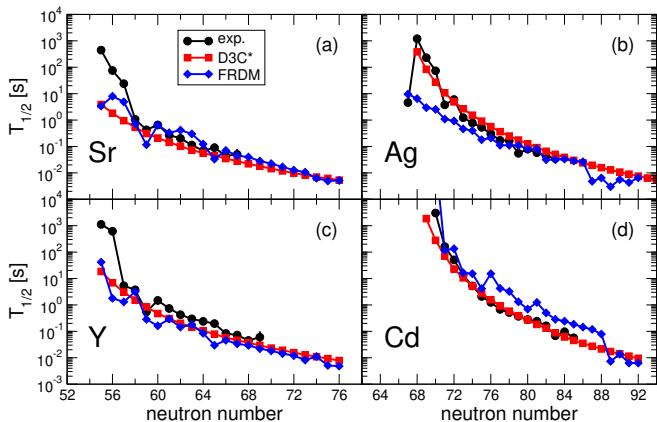
Structure Gamow-Teller strength

- Gamow-Teller strength is characterized by the presence of a resonance at excitation energies around 10-15 MeV.
- With increasing neutron-excess a larger fraction of strength is in the decay window.
- Low-lying strength is rather sensitive to correlations.



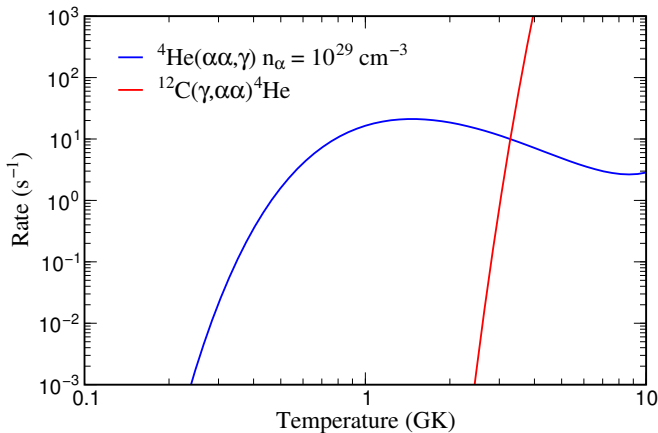
Systematics half-lives

Half-lives decrease with neutron excess.



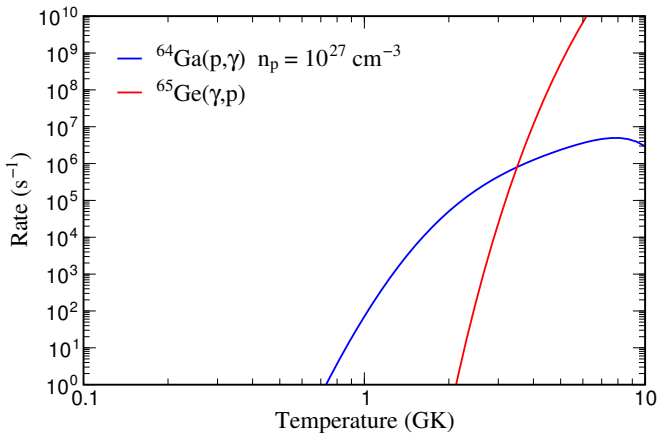
T. Marketin, L. Huther, and G. Martínez-Pinedo, Phys. Rev. C **93**, 025805 (2016).

Rate Examples: ${}^4\text{He}(\alpha\alpha, \gamma)$

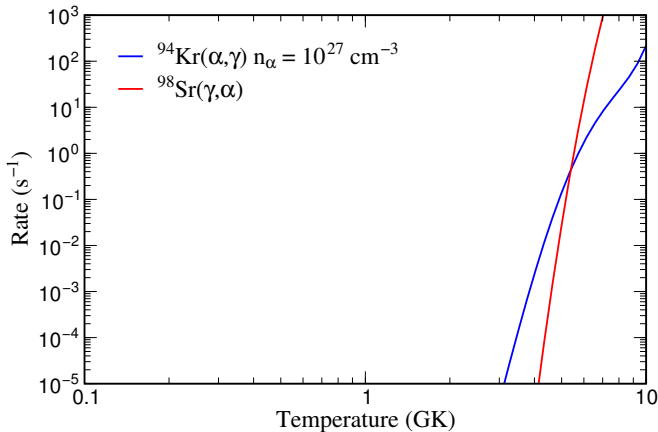




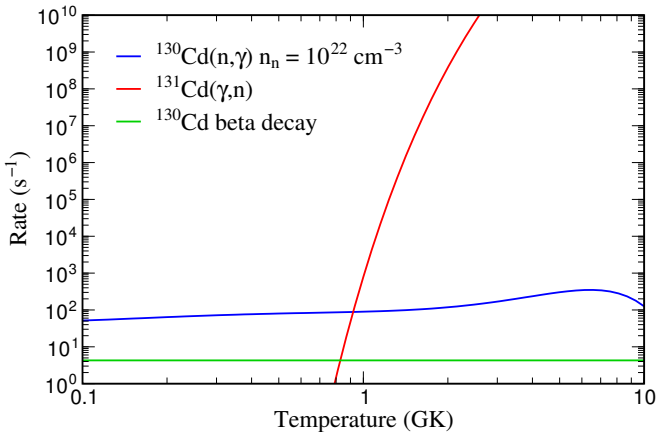
Rate Examples: (p, γ)



Rate Examples: (α, γ)

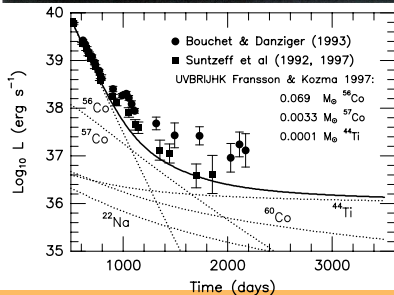
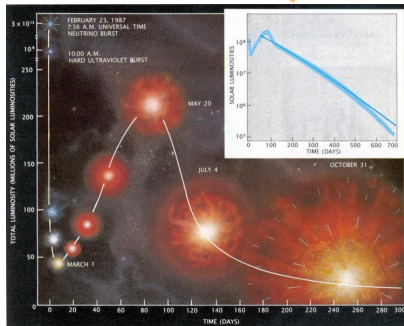
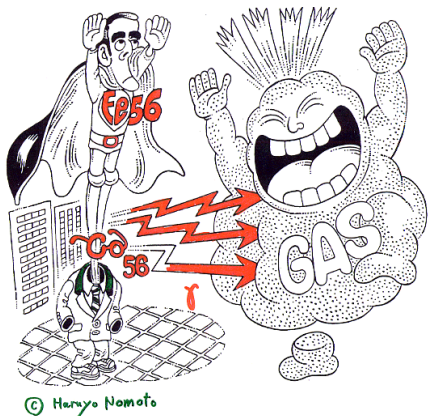


Rate examples: (n, γ)

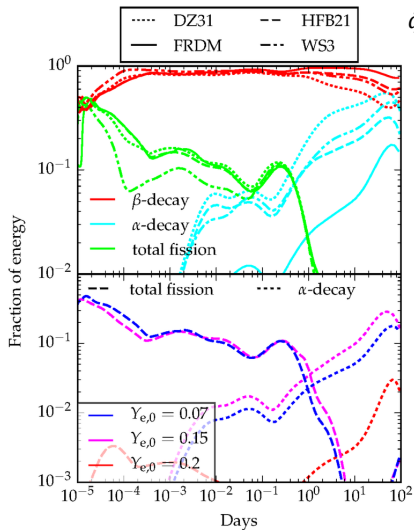


Electromagnetic signatures of nucleosynthesis

Supernova light curves follow the decay of ^{56}Ni ($t_{1/2} = 6$ d) and later ^{56}Co ($t_{1/2} = 77$ d)



Energy production and thermalization

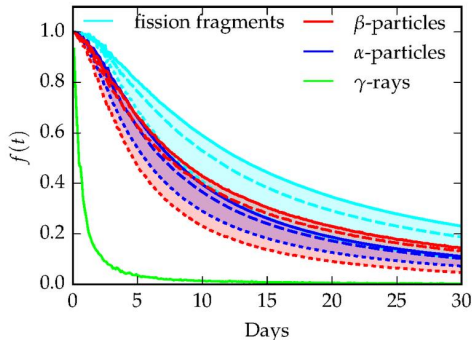


$$\dot{q}(t) = \sum_k f_k(t) \dot{\epsilon}_k(t)$$

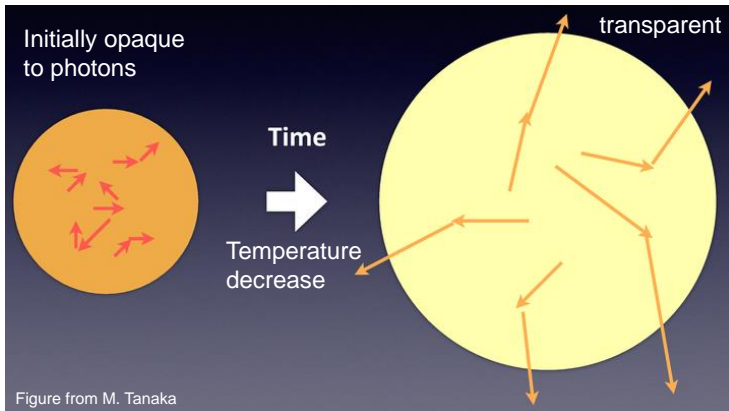
$\dot{\epsilon}_k(t)$ energy emitted in particle k

$f_k(t)$ thermalization efficiency particle k

Thermalization depends on particle, ejecta dynamics, magnetic field, ...



See Barnes, Kasen, Wu, GMP, ApJ 829, 110 (2016); Kasen & Barnes, arXiv:1807.03319



The transition from an opaque to transparent regime depends on the interaction probability of the photons (opacity). Depends on the structure of the atoms.

Low opacity: early emission from hot material at short wavelengths (blue)

High opacity: late emission from colder material at longer wavelengths (red)

Light curve is expected to peak when photon diffusion time is comparable to elapsed time (Metzger et al 2010, Kasen et al 2017)

$$t_{\text{diff}} = \frac{\rho \kappa R^2}{3c}, \quad \rho = \frac{M}{4\pi R^3/3}, \quad R = vt$$

$$t_{\text{peak}} \approx \left(\frac{\kappa M}{4\pi c v} \right)^{\frac{1}{2}} \approx 1.5 \text{ days} \left(\frac{M}{0.01 M_{\odot}} \right)^{\frac{1}{2}} \left(\frac{v}{0.01c} \right)^{-\frac{1}{2}} \left(\frac{\kappa}{1 \text{ cm}^2 \text{ g}^{-1}} \right)^{\frac{1}{2}}$$

The Luminosity is $L(t) \approx M \dot{\epsilon}(t)$, $\dot{\epsilon}(t) \approx 10^{10} \left(\frac{t}{1 \text{ day}} \right)^{-\alpha} \text{ erg s}^{-1} \text{ g}^{-1}$

$$L_{\text{peak}} \approx 1.1 \times 10^{41} \text{ erg s}^{-1} \left(\frac{M}{0.01 M_{\odot}} \right)^{1-\frac{\alpha}{2}} \left(\frac{v}{0.01c} \right)^{\frac{\alpha}{2}} \left(\frac{\kappa}{1 \text{ cm}^2 \text{ g}^{-1}} \right)^{-\frac{\alpha}{2}}$$

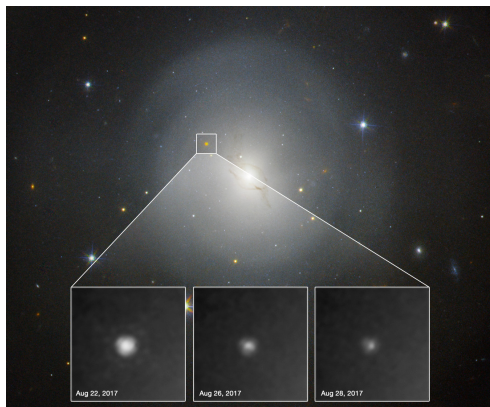
Very sensitive to atomic opacity

$\kappa \approx 1 \text{ cm}^2 \text{ g}^{-1}$, light r process material (blue emission)

$\kappa \approx 10 \text{ cm}^2 \text{ g}^{-1}$, heavy (lanthanide/actinide rich) r process (red emis.)

AT 2017 gfo: electromagnetic signature from r process

In-situ signature of r process nucleosynthesis

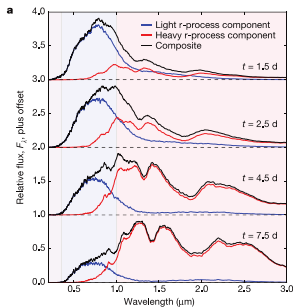


NASA and ESA. N. Tanvir (U. Leicester), A. Levan (U. Warwick), and A. Fruchter and O. Fox (STScI)

- Novel fastly evolving transient
- Signature of statistical decay of freshly synthesized r process nuclei

Two components model

Kasen et al, Nature 551, 80 (2017)

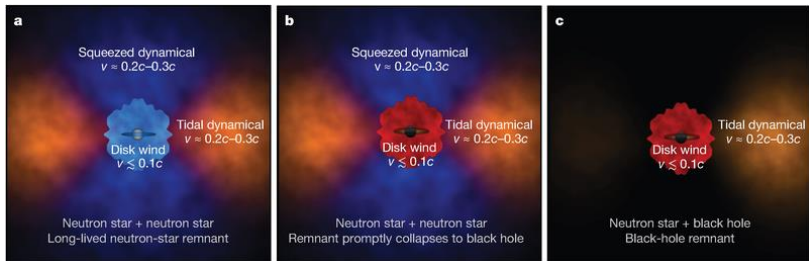


- Blue component from polar ejecta subject to strong neutrino fluxes (light r process)

$$M = 0.025 M_{\odot}, v = 0.3c, X_{\text{lan}} = 10^{-4}$$

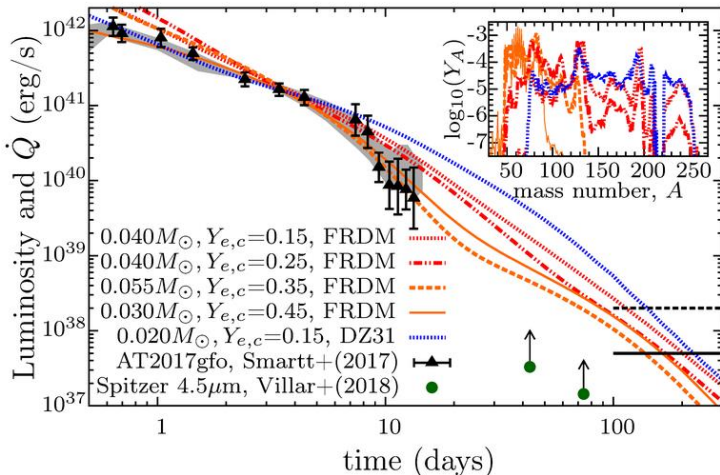
- Red component disk ejecta after NS collapse to a black hole (includes both light and heavy r process)

$$M = 0.04 M_{\odot}, v = 0.15c, X_{\text{lan}} = 10^{-1.5}$$



Nuclear fingerprints light curve

Can we identify particular nuclear signatures in the light curve?



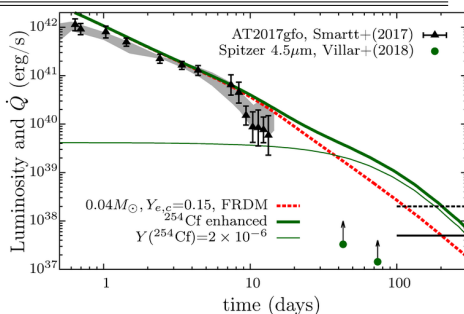
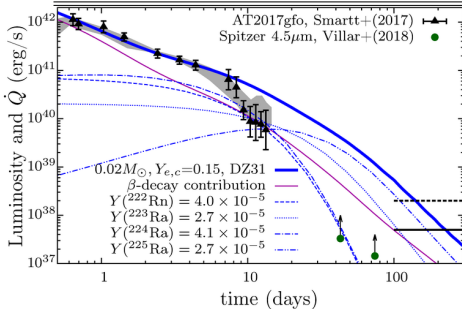
Observations between 10 and 100 days are sensitive to composition.
Light curve becomes dominated by individual decays

Wu, Barnes, GMP, Metzger, PRL 122, 062701 (2019)

Signature dominating decay chains

Isotope	Decay channel	$t_{1/2}$ (d)	Q (MeV)	E_α (MeV)	E_e (MeV)	E_γ (MeV)
^{224}Ra	$\alpha\beta^-$ to ^{208}Pb	3.6319(23)	30.875	26.542	0.891	1.474
^{222}Rn	$\alpha\beta^-$ to ^{210}Pb	3.8215(2)	23.826	19.177	0.949	1.715
^{225}Ra	β^-	14.9(2)	0.356	-	0.097	0.012
^{225}Ac	$\alpha\beta^-$ to ^{209}Bi	10.0(1)	30.196	27.469	0.632	0.046
^{223}Ra	$\alpha\beta^-$ to ^{207}Pb	11.43(5)	29.986	26.354	0.937	0.304

Isotope	Decay channel	$t_{1/2}$ (d)	Q (MeV)	E_{Kinetic} (MeV)	E_n (MeV)	E_γ (MeV)
^{254}Cf	Fission	60.5(2)	-	185(2)	-	-



Decline observed light curve at 10 days suggest an upper limit of $0.01 M_\odot$ of U and Th
 Wu, Barnes, GMP, Metzger, , PRL 122, 062701 (2019)

